Uncovering Early Galaxy Evolution in the ALMA and JWST Era
Proceedings IAU Symposium No. 352, 2019
E. da Cunha, J. Hodge, J. Afonso, L. Pentericci & D. Sobral, eds.

doi:10.1017/S1743921319009116

ALPINE: The ALMA [*CII*] survey of normal star-forming galaxies at $4 < z < 6$

Olivier Le Fèvre[1], Matthieu Bethermin[1], Andreas Faisst[2], P. Capak[2], P. Cassata[3], J. D. Silverman[4], D. Schaerer[5], L. Yan[2] and the ALPINE team[6]

[1]Aix Marseille Université, CNRS, LAM (Laboratoire d'Astrophysique de Marseille) UMR 7326, 13388, Marseille, France
emails: olivier.lefevre@lam.fr, matthieu.bethermin@lam.fr

[2]IPAC, California Institute of Technology, 1200 East California Boulevard, Pasadena, CA 91125, USA
emails: afaisst@ipac.caltech.edu, capak@ipac.caltech.edu, lyan@ipac.caltech.edu

[3]INAF Osservatorio di Padova and Dipartimento di Fisica e Astronomia, Università di Padova, Vicolo dell'Osservatorio, 3 35122 Padova, Italy
email: paolo.cassata@unipd.it

[4]Kavli Institute for the Physics and Mathematics of the Universe, The University of Tokyo, Kashiwa, Japan 277-8583 (Kavli IPMU, WPI)
email: john.silverman@ipmu.jp

[5]CNRS and Geneva Observatory, University of Geneva, ch. des Maillettes 51, CH-1290 Versoix, Switzerland
email: Daniel.Schaerer@unige.ch

[6]ALPINE team: R. Amorin, S. Bardelli, Boquien, A. Cimatti, M. Dessauges-Zavadsky, Seiji Fujimoto, Ginolfi, M., Hemmati, S., Ibar , G. Jones, A. Koekemoer, G. Lagache , B. Lemaux, R. Maiolino, P. Oesch, Pozzi, Riechers, M. Talia, L. A. M. Tasca, R. Thomas, L. Vallini, D. Vergani, F. Walter, G. Zamorani, and E. Zucca

Abstract. The ALMA-ALPINE [CII] survey (A2C2S) aims at characterizing the properties of normal star-forming galaxies (SFGs) observed in the [CII]-158μm line in the period of rapid mass assembly at redshifts $4 < z < 6$. Here we present the survey and the selection of 118 galaxies observed with ALMA, selected from large samples of galaxies with spectroscopic redshifts derived from UV-rest frame. The observed properties derived from the ALMA data are presented and discussed in terms of the overall detection rate in [CII] and far-IR continuum. The sample is representative of the SFG population at these redshifts. The overall detection rate is 61% down to a flux limit of 0.07 mJy. From a visual inspection of the [CII] data cubes together with the large wealth of ancillary data we find a surprisingly wide range of galaxy types, including 32.4% mergers, 25.7% extended and dispersion dominated, 13.5% rotating discs, and 16.2% compact, the remaining being too faint to be classified. ALPINE sets a reference sample for the gas distribution in normal star-forming galaxies at a key epoch in galaxy assembly, ideally suited for studies with future facilities like JWST and ELTs.

Keywords. Galaxies: high redshift – Galaxies: formation – Galaxies: star formation

1. Introduction

The mass assembly in galaxies at different epochs proceeds from several physical processes which, together, produce the remarkable observed evolution of the star formation rate density (SFRD) with cosmic time (Silk & Mamon (2012); Madau & Dickinson (2014); Dayal & Ferrara (2018)). The SFRD first rises during the reionization epoch, to reach a

peak at $z \sim 2-3$ after a ∼1 dex increase in ∼3 Gyr, then decreases by ∼0.8 dex in ∼10 Gyr to the current time (Madau & Dickinson (2014); Bouwens *et al.* (2015)). Along with star formation, the total stellar mass density (SMD) in galaxies is observed to rise steeply from early times to $z \sim 2$, followed by a slower increase at $z < 2$ Ilbert *et al.* (2013).

At the root of the SFRD and SMD evolution, the transformation of gas into stars in a hierarchical picture of galaxy assembly is a key element. Two main processes are shown from more and more detailed simulations to drive this evolution: gas accretion and galaxy-galaxy merging . This is expected to be tempered by feedback processes from gas expelled from galaxies by strong AGN and/or stellar jets and winds. While this is appealing from a theoretical and simulation standpoint, there is actually very little observational support towards a comprehensive, consistent, and quantitative picture, particularly at early cosmic epochs when mass assembly is in a major phase. Galaxy mergers are observed at all epochs, with a major merger rate increasing to $z \sim 2$ possibly flattening to $z \sim 4-5$, while gas accretion suffers from weak signatures difficult to identify observationally. On the other hand, feedback processes are directly measured e.g. Le Fèvre *et al.* (2019), and thought to affect both the bright (AGN) and faint end of the galaxy luminosity function (LF) Croton (2006).

To disentangle the relative contributions of these processes, the far infrared (FIR) domain redshifted in the sub-mm for high-z galaxies is proving particularly rich. From the sub-mm it is now possible to investigate the properties of star-forming galaxies up to the epoch of HI reionisation. The [CII]-158μm line is the dominant coolant making it one the strongest FIR lines. The primary [CII] emission is from photo-dissociation regions (PDR) and cold neutral medium (CNM) of molecular clouds. [CII] at high-z has raised considerable interest as it probes the gas from which stars form in normal galaxies, and then broadly traces star formation activity, offering an important window on galaxy formation Carilli & Walter (2013). This led to the detection of strong [CII] emitters, up to very high redshifts Capak *et al.* (2015), an easier measurement than the FIR continuum. Searching for [CII] emission, interpreting and simulating the observations, and comparing with other line emission like Lyman-α, has therefore become a major new way of studying high-z galaxies. The strong UV radiation in high-z galaxies results in a non-negligible fraction of [CII] emission from the extended warm ISM. The evolution of [CII] emission and its resolved velocity profile provide important information on the SFR and ISM properties, setting constraints on the dynamical and gas masses of galaxies. The morphology of the [CII] emission indicates if star formation is compact or extended, an important element to understand high-z star formation . Beyond the line flux, the FIR continuum emission adjacent to [CII] is near the peak of the FIR emission. It constrains the total FIR luminosity, and provides a good measure of the total SFR when combined with UV continuum measurements. The continuum flux can also be combined with UV colors and luminosity to construct the Infrared-Excess (L_FIR/L_UV, so-called IRX) vs. UV color (β) diagnostic, providing insight into the spatial distribution of dust, dust grain properties, and metallicity.

Simulations of forming galaxies during and right after reionization are informing on the possible properties of these galaxies despite the difficulty to take into account early galaxy formation processes during and right after the EoR in a consistent way. Specific predictions related to [CII] emission are useful to guide and compare to observations.

This whole domain opened up at high redshift $z > 4$ with ALMA becoming fully operational, when it was realized from pilot observations that detecting [CII] for normal galaxies was ubiquitous even with short on-source exposure times Capak *et al.* (2015). Galaxies with star formation rates as low as a few $M_\odot.yr^{-1}$ have been reported at $z \sim 5$ Capak *et al.* (2015), and [CII] is now detected for galaxies well into the reionisation epoch.

https://doi.org/10.1017/S1743921319009116 Published online by Cambridge University Press

However, existing observations of [CII] in normal galaxies at these epochs are still scarce. While strong sub-mm sources have been primarily targeted, they provide a view biased towards the highly star-forming population with SFR$>1000\ M_{\odot}.yr^{-1}$. Normal galaxies, that is galaxies with SFR~ 10 to a few hundred, lying on the so-called main sequence at these redshifts Khusanova *et al.* (2019), have not been observed in statistically representative numbers. The Capak *et al.* (2015) observations proved that this was feasible and prompted us to submit the ALPINE Large Program, largely designed based on the properties of the Capak *et al.* (2015) sample. A key element was the availability of large samples of these normal galaxies, with accurate *spectroscopic redshifts* to be able to define ALMA observations with a high success rate in detecting [CII].

In these proceedings, we present the sample selection as in the original proposal. We give an overview of the ALMA observations. We then describe the main properties of the sample, including the redshift distribution, detection rates in [CII] and continuum, and observed flux limits. We give examples of maps of sample galaxies in the [CII] line.With these maps, kinematic data, and all ancillary imaging data we perform an empirical visually-based morpho-kinematic classification.

2. Sample selection

The sample is drawn from large spectroscopic survey samples of normal SFGs in the COSMOS and ECDFS fields.

A key element is that galaxies must have a reliable spectroscopic redshift in $4.4 < z_{spec} < 5.8$ ($< zspec > \sim 4.7$, excluding $4.65 < z < 5.05$ where [CII] falls in a low transmission atmospheric window). Galaxies are UV-selected with $L_{UV} > 0.6L^*$ to include most of the star formation traced by the UV, and excluding AGN. Accurate redshifts come from extensive spectroscopic campaigns at the VLT Le Fèvre *et al.* (2015) and Keck Hasinger *et al.* (2018), unbiased against Lyman-α emitters or absorbers. The absolute UV luminosity cut ($M_{UV} < -20.2$) is equivalent to SFR$>10\ M_{\odot}/yr$. Using the relation for high-z galaxies Capak *et al.* (2015), this SFR limit is equivalent to $L[CII] > 1.2 \times 10^8 L_{\odot}$. This sample is representative of the overall SFG population, rather than ULIRGS, that is with galaxies essentially positioned on or near the so-called main sequence in the SFR versus M_{star} plane observed at these redshifts (Tasca *et al.* (2015), Khusanova *et al.* (2019)).

3. ALMA observations

This program was awarded an ALMA Large Program status under number 2017.1.00428.L for a total of 69 hours. ALMA observations were carried out in Band-7 starting in May 2018 during Cycle 5 and completed in February 2019 in Cycle 6. Each target was observed for about 30 minutes and up to one hour of on-source integration time, pointing at the rest-frame UV positions of the sources. The availability of spectroscopic redshifts allowed to accurately set the main spectral window on the expected [CII] frequencies. The other side-band was then used for FIR continuum measurements.

At these redshifts, the velocity width of one ALMA bandpass in band-7 is as narrow as ∼3000 km/s. Samples with photometric redshifts accurate to $\sim 0.05 \times (1+z)$ Ilbert *et al.* (2013), would have added a considerable uncertainty on the detection of [CII] and associated incompleteness, making it more hazardous to build e.g. the [CII] luminosity function. With an accuracy of a few hundred km/s even at low spectral resolution from optical (UV rest-frame) spectroscopy Le Fèvre *et al.* (2015), the availability of z_{spec} is therefore a key element of this program ensuring a high [CII] detection rate and, for those galaxies which would be undetected, setting stringent upper limits.

We use the TDM mode of the ALMA correlator, which offers the largest bandwidth to optimize the continuum sensitivity. The resolution varies with redshift from 26 to 35

https://doi.org/10.1017/S1743921319009116 Published online by Cambridge University Press

km/s. We assumed 235 km/s FWHM line width (or sigma ∼100 km/s), which is the average width measured in the Capak *et al.* (2015) sample. Emission lines were thus expected to be spectrally resolved giving the possibility to measure the line width when the SNR is sufficient.

We privilege detection over spatial and spectral resolution, and with the typical size of the Capak *et al.* (2015) sources being 0.5-0.7 arcsec, we elected to use ALMA array configurations offering an angular resolution not larger than 0.7 arcsec. The median beam size of the ALMA observations is then about 0.7 arcsec FWHM.

4. Detection rate

The Signal to noise ratio (SNR) obtained on the [CII] line detection has a median $SNR \simeq 6.2$. See Béthermin *et al.* (2019, in prep.) for more details. Taking 3.5σ as a conservative detection limit, ALPINE detected [CII] in 73 galaxies over 118, hence a success rate of ∼62%. In the continuum adjacent to [CII], 25 galaxies, or 21%, are detected. These rates are quite impressive given the redshift of the sources and relatively short integration times. The SNR in [CII] of most other targets varies in the range from 0.5 to 3, providing useful upper limits.

5. [CII] maps and morpho-kinematic classification

Example images in the [CII] line of sources with [CII] detected at more than 3.5σ are presented in Fig. 1.

These images give a first view of the shape of the [CII] emission in normal galaxies at $4 < z < 6$. There are several facts worth noting. Even though the observations were carried out with a beam size providing moderate spatial resolution with FWHM∼0.7 arcsec, about two third of the sources are resolved in [CII]. This means that intrinsic (total) sizes must be reaching several kilo-parsecs. By itself this fact gives an indication that physical processes at work in those galaxies are puffing up their sizes beyond being compact. Another striking evidence from these images is the large diversity of [CII] emission morphology. Some objects appear as very extended, some others with double merger-like components while others are compact (unresolved). This diversity must also reflect a diversity in the physical processes at work.

We perform an empirical visual-based morpho-kinematic classification using the [CII] maps the velocity and spectral information in the 3D cubes and all optical and NIR ancillary data. We find 32.4% of galaxies in the merger class 2, 25.7% in the extended and dispersion dominated class 3, 13.5% rotating discs in class 1, and 16.2% compact in class 4, the rest of the sample being too difficult to classify (class 5). We note the high fraction of mergers, indicating that mass assembly through merging is frequent at these redshifts for normal main sequence SFGs. Preliminary examination of spatial and velocity information indicates that most merging systems would merge within 0.5 to 1 Gyr (see the triple merger system presented in Jones *et al.* (2019)), which then means that most of these mergers would end-up forming one single galaxy by $z \sim 2.5$.

6. Conclusions

The ALMA-ALPINE [CII] survey (A2C2S) provides an unprecedented view of a representative sample of 118 star-forming galaxies observed in formation right after the end of HI reionisation at redshifts $4 < z < 6$. Galaxies are selected on the basis of an existing reliable spectroscopic redshift, and using the SED-based SFR to predict the [CII] flux using the De Looze *et al.* (2014) relation and selecting SFR such that $L[CII] > 1.2 \times 10^8 L_\odot$. The overall detection rate is 61% for galaxies detected in [CII] 3.5σ above the noise,

https://doi.org/10.1017/S1743921319009116 Published online by Cambridge University Press

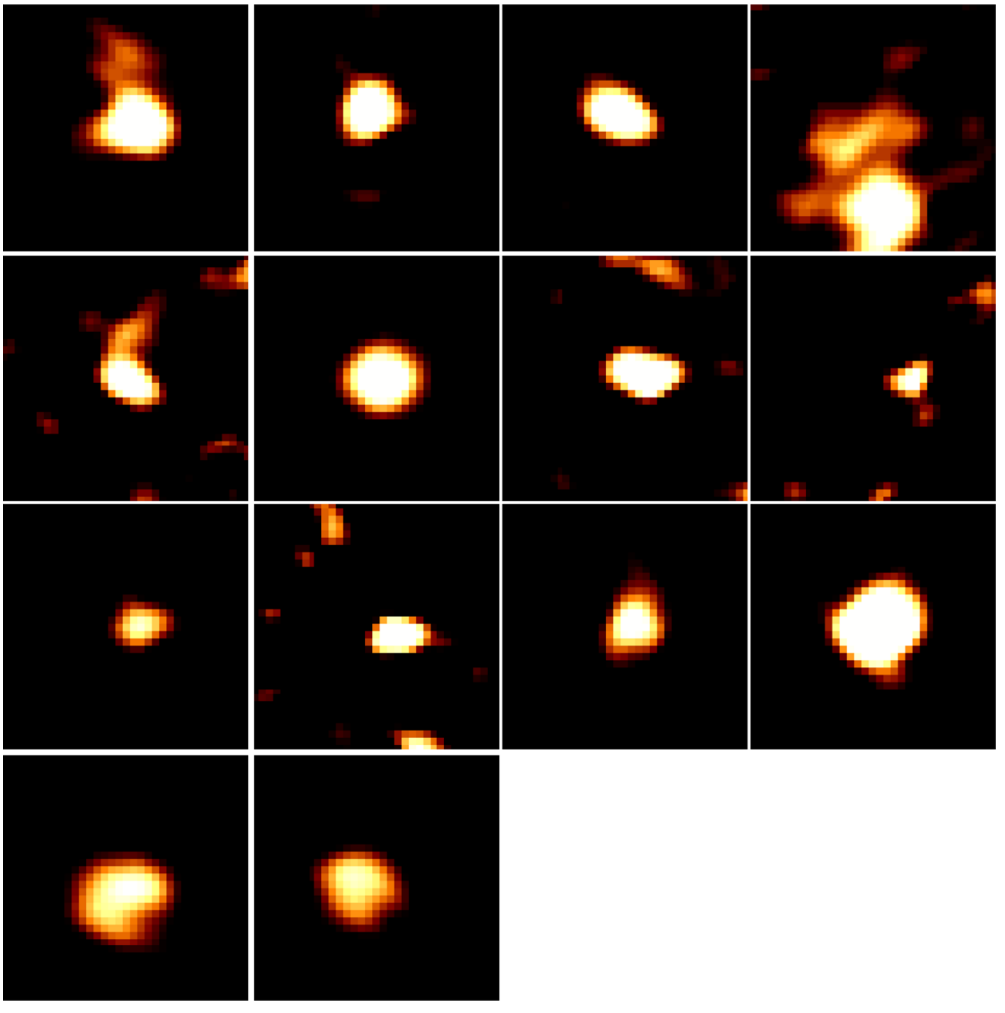

Figure 1. [CII] 'moment 0' maps obtained from projecting the ALPINE cubes along all frequencies corresponding to ±1500 km/s around the peak [CII] flux, unless cut by the edge of the ALMA bandpass (see text). Each panel is 5×5 arcsec^2 or about 6 kpc on a side at the mean redshift of the survey. From top to bottom, left to right, objects vuds-cosmos-5100822662, vuds-cosmos-5100969402, vuds-cosmos-5100994794, vuds-cosmos-5101209780, vuds-cosmos-5101210235, vuds-cosmos-5101218326, vuds-cosmos-5101244930, vuds-cosmos-5101288969, vuds-cosmos-510596653, uds-cosmos-510605533, vuds-cosmos-510786441, uds-cosmos-5110377875, vuds-cosmos-5180966608, vuds-efdcs-530029038. These images show the large range of morpholopy in[CII], from compact to extended and resolved or merger-like.

down to a flux limit of 0.07 mJy. projected. Combining projected [CII] 'moment zero' maps with velocity channel maps, velocity field, and all available ancillary information, we establish a classification scheme. We find a surprisingly wide range of galaxy types, including 32.4% mergers, 25.7% extended and dispersion dominated, 13.5% rotating discs, and 16.2% compact, the remaining being too faint to be classified. This diversity of types indicates that several physical processes are at work to assemble mass in these galaxies, first and foremost galaxy-galaxy merging.

https://doi.org/10.1017/S1743921319009116 Published online by Cambridge University Press

References

Bouwens, R. J., Illingworth, G. D., Oesch, P. A., *et al.* 2015, Ap.J., 803, 34
Capak, P. L., Carilli, C., Jones, G., *et al.* 2015, Nature, 522, 455
Carilli, C. L. & Walter, F. 2013, Annual Review, Astronomy and Astrophysics, 51, 105
Croton, D. J. 2006, MNRAS, 369, 1808
Dayal, P. & Ferrara, A. 2018, Physics Review, 780, 1
De Looze, I., Cormier, D., Lebouteiller, V., *et al.* 2014, A&A, 568, A62
Hasinger, G., Capak, P., Salvato, M., *et al.* 2018, Ap.J., 858, 77
Ilbert, O., McCracken, H. J., Le Fèvre, O., *et al.* 2013, A&A, 556, A55
Jones, G. C., Bethermin, M., Fudamoto, Y., *et al.* 2019, arXiv e-prints, arXiv:1908.07777
Khusanova, Y., Le Fèvre, O., Cassata, P., *et al.* 2019, arXiv e-prints, arXiv:1903.01884
Le Fèvre, O., Tasca, L. A. M., Cassata, P., *et al.* 2015, A&A, 576, A79
Le Fèvre, O., Lemaux, B. C., Nakajima, K., *et al.* 2019, A&A, 625, A51
Madau, P. & Dickinson, M. 2014, Annual Review, Astronomy and Astrophysics, 52, 415
Silk, J. & Mamon, G. A. 2012, Research in Astronomy and Astrophysics, 12, 917
Tasca, L. A. M., Le Fèvre, O., Hathi, N. P., *et al.* 2015, A&A, 581, A54

https://doi.org/10.1017/S1743921319009116 Published online by Cambridge University Press